Thermochimica Acta, 222 (1993) 91–103
Elsevier Science Publishers B.V., Amsterdam

Thermal transformations of $NH_4M^{II}PO_4 \cdot H_2O$ (where M^{II} is Mg, Mn, Co, Cu)

J. Pysiak [a,*], E.A. Prodan [b], V.V. Samuskevich [b], B. Pacewska [a] and N.A. Shkorik [b]

[a] *Institute of Chemistry, Płock Branch of Warsaw University of Technology, 09-400 Płock (Poland)*
[b] *Institute of General and Inorganic Chemistry, Belorussian Academy of Sciences, 220072 Minsk (Belarus)*

(Received 22 October 1992)

Abstract

Isothermal and non-isothermal transformations of polycrystalline $NH_4M^{II}PO_4 \cdot H_2O$ (where M^{II} is Mg, Mn, Co, Cu) in atmospheres of various gases (open air, humid air, H_2O vapour, $p_{H_2O} = 20$ hPa, gaseous NH_3, $p_{NH_3} = 5–925$ hPa, vacuum, $p = 10^{-5}$ hPa) were studied by DTA, TG, DTG, XRD, PC, and chemical analyses at 20–950°C. The kinetic characteristics of the evolution of gaseous products and of the essential processes of dehydration and deammoniation, and the anionic rearrangements are considered.

INTRODUCTION

Compounds of the type $NH_4M^{II}PO_4 \cdot H_2O$ (where M^{II} is Mg, Mn, Co, or Cu) on heating may undergo several types of transformation including: thermal decomposition of the crystal hydrate with evolution of crystallization water and formation of anhydrous salt in a crystalline or amorphous state

$$NH_4M^{II}PO_4 \cdot H_2O \rightarrow NH_4M^{II}PO_4 + H_2O\uparrow \qquad (1)$$

destruction of the complex ammonium cation with formation of gaseous ammonia and formation of an acid salt.

$$NH_4M^{II}PO_4 \rightarrow M^{II}HPO_4 + NH_3\uparrow \qquad (2)$$

or rearrangement of the acid salt anion with evolution of the remaining

---

* Corresponding author.

water molecule and formation of diphosphate as the end product

$$2M^{II}HPO_4 \rightarrow M_2^{II}P_2O_7 + H_2O\uparrow \qquad (3)$$

Reaction (1) prevails when $NH_4M^{II}PO_4 \cdot H_2O$ is heated in an atmosphere of gaseous NH_3, which suppresses reaction (2) and enables the elimination of crystallization water without the loss of ammonia [1,2]. Thus, heating $NH_4CoPO_4 \cdot H_2O$ in NH_3 atmosphere at 180°C gives the low-temperature crystalline form of NH_4CoPO_4-bt, whereas heating at 260°C gives the high-temperature form of NH_4CoPO_4-**I** [1,3]. Reaction (2) results in the formation of an amorphous product, whereas reaction (3) yields an anionic rearrangement, which proceeds through additional stages of formation of tri-, tetra-, and pentaphosphates, and higher phosphates, all of which are converted into diphosphate at the end of gas evolution [4–7].

Analysis of the literature data [1–12] (a more complete list of papers dealing with this problem and including papers published in Russian is given in monographs 13 and 14) shows that reactions (1)–(3) may replace each other depending on the nature of the starting materials, their dispersion degree, the rate of non-isothermal heating, the duration of heating at the temperature, the composition and pressure of the surrounding gas atmosphere, and other factors.

In order to determine the contributions of reactions (1)–(3) to the overall process, the aim of this work was to provide conclusive data on the isothermal and non-isothermal transformations of polycrystalline samples of $NH_4M^{II}PO_4$ (where M^{II} is Mg, Mn, Co, Cu) in air, in vacuum, and in the atmosphere of the gaseous reaction products—water vapour and ammonia. In addition to the determination of the total gases evolved (gravimetrically from the mass loss $\Delta m_{H_2O+NH_3}$), the losses of ammonia Δm_{NH_3} and water Δm_{H_2O} were determined separately. The amount of ammonia evolved was determined by periodic analyses of the solid residue and by determination of NH_3 in the mixture of gases evolved; Δm_{H_2O} was calculated from the difference between $\Delta m_{H_2O+NH_3}$ and Δm_{NH_3}.

EXPERIMENTAL

Polycrystalline $NH_4M^{II}PO_4 \cdot H_2O$ was obtained by the well-known method [13] of precipitation from aqueous solutions of $(NH_4)_2HPO_4$ (analytical grade) and of soluble salts of the divalent metals, in molar ratios of (1.3–3.0):1 at 20°C (M^{II} = Mn or Cu), 70°C (M^{II} = Co) or 90°C (M^{II} = Mg). The soluble salts used were $MgCl_2$, $MnCl_2$, $CuCl_2$, and $CoSO_4$, all of analytical grade. After separation from the mother liquor, the precipitates were dried for 2–3 days at room temperature in air at 60% relative humidity and then analysed. The divalent metals were determined complexometrically: nitrogen, by the Kjeldahl method; phosphorus, by the photocolorimetric method; and water, by calculation from the loss of mass on roasting $\Delta m_{H_2O+NH_3}$, after subtraction of Δm_{NH_3}. The composition determined experimentally was very near to that found by calculation. The X-ray diffraction characteristics and IR absorption spectra corresponded to those found in the literature for $NH_4M^{II}PO_4 \cdot H_2O$ (where M^{II} is Mg, Mn, Co, and Cu) [15, 16]. The samples were microcrystalline powders with the following grain size and shape: $NH_4MgPO_4 \cdot H_2O$, 0.05–0.1 mm, prisms; $NH_4MnPO_4 \cdot H_2O$, 0.05–0.1 mm, platelets; $NH_4CoPO_4 \cdot H_2O$, 0.1–0.2 mm, flat prisms; $NH_4CuPO_4 \cdot H_2O$, 0.05–0.1 mm, long prisms.

In non-isothermal experiments performed in air atmosphere, we used a 3434-C derivatograph with a microprocessor control (platinum sample holder of open type, sample weight $m = 100$ mg, heating rate 10 K min^{-1}). In both the isothermal and non-isothermal experiments in vacuum, in water vapour or in gaseous ammonia, a quartz microbalance (sensitivity 0.5 mg mm^{-1}, sample mass 50–70 mg, flat-bottomed Pt sample holder, in which the sample was spread as a thin layer) was used. The sample with the holder was suspended in the quartz spiral, the system was evacuated, and the experiment was started immediately at a heating rate 2.5–5.0 K min^{-1} (when heating in vacuum), or the system was filled with water vapour or dry gaseous ammonia to the pressure required before the heating was started (when heating in a gas atmosphere).

In the isothermal experiment, the holder with the sample was introduced through a ground-joint gate to the thermostated compartment of the reaction vessel and kept a constant temperature (±0.5°C). In both isothermal and non-isothermal heating, the pressure in the system was kept constant within the range of $p = (1 \pm 3) \times 10^{-5}$ hPa, due to the freezing-cut of the gas evolved during the reaction, with $p_{H_2O} = (20 \pm 1) \times 10^{-5}$ hPa, $p_{NH_3} = (5 \pm 1)$ hPa and $p_{NH_3} = (925 \pm 5)$ hPa.

In a separate series of experiments, where the heating was broken for sampling, the conditions of heating and pressure were the same but the sample weight was $m = 150$–200 mg, and samples were prepared for X-ray diffraction analyses (DRF diffractometer-2.0; Cu Kα radiation; internal standard, NaCl). Both these and the other samples were subjected to chemical and chromatographic analysis. The anionic composition was determined by quantitative ascending chromatography using FN12 chromatographic paper. The interfering effect of M^{2+} cations on the chromatographic process was eliminated by addition of EDTA or by treatment of the solution with KU-2 cation exchange resin in the Na^+ form.

The same high-vacuum setup and identical experimental conditions were applied in determination of the kinetic curves of dehydration, Δm_{H_2O} versus τ (τ is time), and deammoniation, Δm_{NH_3} versus τ. The only difference was that the gas evolved was frozen out into small vessels of capacity 8–10 cm^3, filled with a known volume of aqueous HCl. The vessels were periodically connected with the apparatus and cooled with liquid nitrogen. The solutions of HCl were titrated and the results were plotted in Δm_{NH_3}–τ coordinates. The difference between $\Delta m_{H_2O+NH_3}$ obtained gravimetrically and Δm_{NH_3} was utilized in drawing the plot of Δm_{H_2O}–τ.

In cases where the samples were heated in water vapour atmosphere, the kinetic curves Δm_{NH_3}–τ were constructed from the results of periodic determinations of ammonia in the solid residue. In a flow-through modification of the high-vacuum setup, air saturated with water vapour (100% humidity) was passed through the apparatus at a rate of 50 ml min^{-1}. At the outlet from the reaction vessel, the air was passed through periodically changed vessels filled with 0.01 N HCl, which was then titrated to determine the amount of absorbed NH_3. Kinetic curves constructed from these data (Δm_{NH_3}–τ) corresponded well with those based on analyses of the solid residue.

RESULTS AND DISCUSSION

Derivatograms of the samples studied are shown in Figs. 1–4. The broken lines represent the values of $\Delta m_{H_2O+NH_3}$ corresponding to reactions (1), (2) and (3). They are in good agreement with derivatographic data obtained with samples of $m = 0.81$–1.35 g [8]. The DTA and DTG curves obtained on heating $NH_4MnPO_4 \cdot H_2O$ have effects with peak temperatures of 226 and 423°C (according to ref. 8, 250 and 400°C). Heating $NH_4CoPO_4 \cdot H_2O$ gave DTA and DTG effects with peak temperatures of 253, 308, 420 and 458°C (220, 340 and 450°C in ref. 8). The TG curve obtained for NH_4CuPO_4 contains, in addition to the final horizontal portion corresponding to completion of reaction (3), an inclined section near $\Delta m_{H_2O+NH_3} = 10\%$ which indicates that reaction (1) can proceed independently of reactions (2) and (3). No such effects were found for other

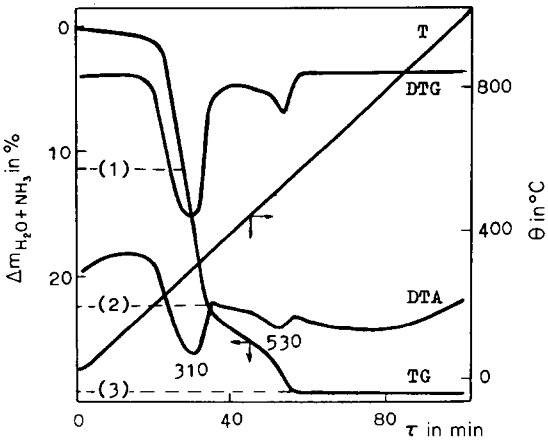

Fig. 1. The derivatogram of $NH_4MgPO_4 \cdot H_2O$, $\Delta m_{H_2O+NH_3} = 29.4\%$.

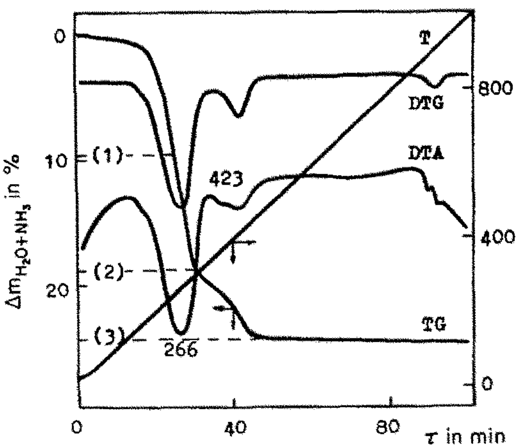

Fig. 2. The derivatogram of $NH_4MnPO_4 \cdot H_2O$, $\Delta m_{H_2O+NH_3} = 25.4\%$.

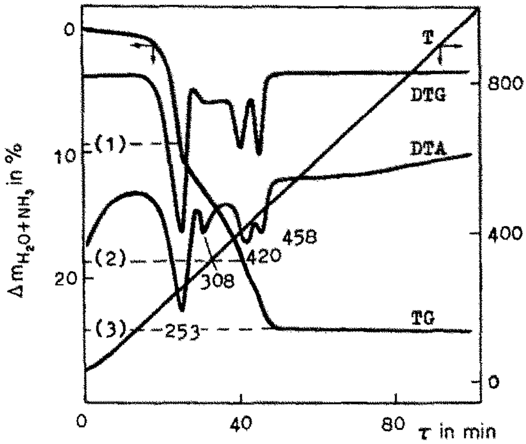

Fig. 3. The derivatogram of $NH_4CoPO_4 \cdot H_2O$, $\Delta m_{H_2O+NH_3} = 24.2\%$.

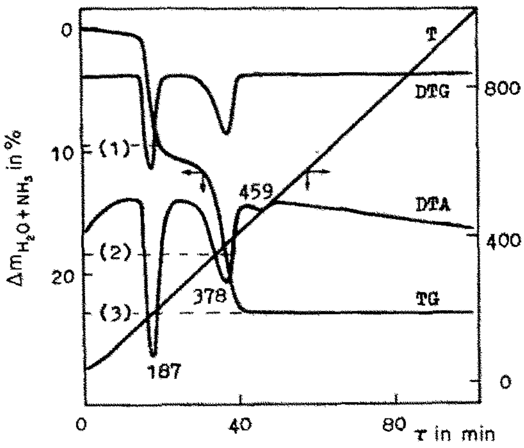

Fig. 4. The derivatogram of $NH_4CuPO_4 \cdot H_2O$, $\Delta m_{H_2O+NH_3} = 22.8\%$.

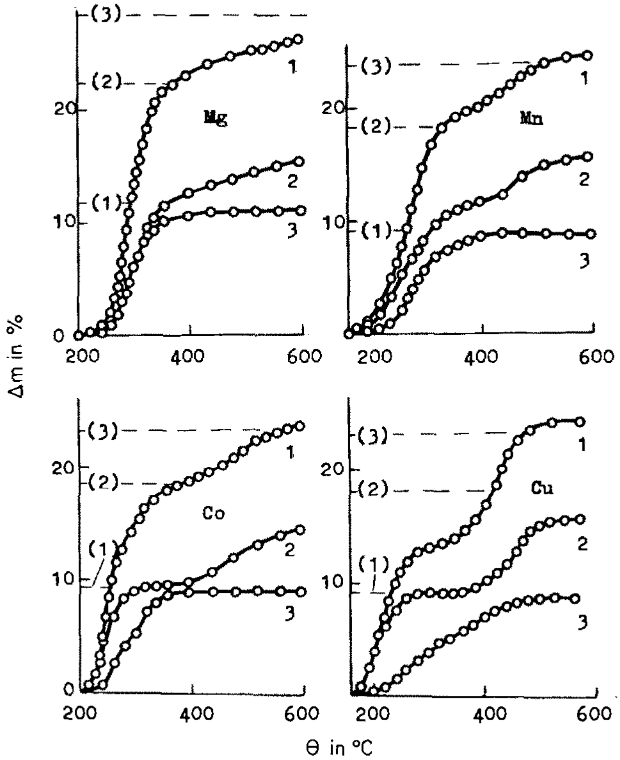

Fig. 5. TG curves of $NH_4M^{II}PO_4 \cdot H_2O$ (where M^{II} is Mg, Mn, Co, Cu) heated in a humid air stream ($v = 50$ ml min^{-1}, RH = 100%, HR = 2.5 K min^{-1}): curve 1, $\Delta m_{H_2O+NH_3}$; curve 2, Δm_{H_2O}; curve 3, Δm_{NH_3}.

samples. Small bends on the TG curves corresponding to $\Delta m_{H_2O+NH_3} = 22.6\%$ (for M^{II} = Mg) and 18.8% (for M^{II} = Mn) may be due to the beginning of anionic condensation.

Thus, the derivatographic data indicate that heating samples of $NH_4M^{II}PO_4 \cdot H_2O$ (where M^{II} is Mg, Mn, or Co) in open air does not, in practise, allow for elimination of the crystallization water without the loss of ammonia. This is also true when heating samples in a stream of air saturated with water vapour at room temperature (Fig. 5). Only the sample of $NH_4CuPO_4 \cdot H_2O$ heated at 200–220°C loses most of its crystallization water with no appreciable loss of ammonia, with a subsequent plateau on the Δm_{H_2O}–τ curve. A similar plateau is seen on curve 2 of $NH_4CoPO_4 \cdot H_2O$, but in this case the loss of ammonia is considerable. Practically simultaneous loss of water and ammonia occurred for $NH_4MgPO_4 \cdot H_2O$, where curves 2 and 3 are inseparable in the temperature range 300–350°C. As when heating in open air, curves 1 for M^{II} = Mn, Co and Cu exhibit inflections corresponding to the beginning of anionic condensation.

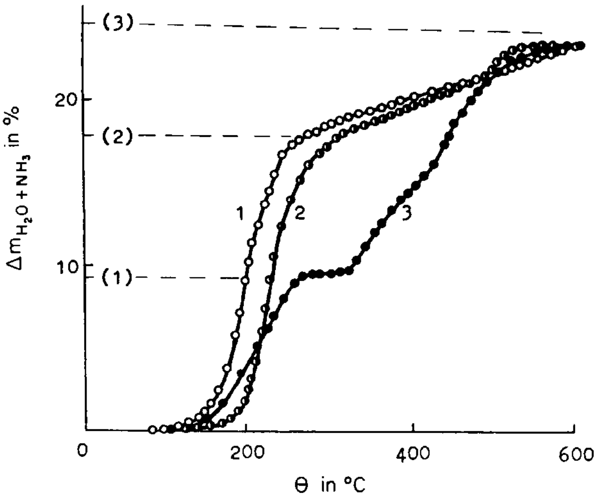

Fig. 6. TG curves of $NH_4CoPO_4 \cdot H_2O$ heated at 2.5 K min^{-1}: curve 1, $p = 10^{-5}$ hPa; curve 2, $p_{H_2O} = 20$ hPa; curve 3, $p_{NH_3} = 136$ hPa.

The separation of reaction (1) from reactions (2) and (3) takes place when the samples are heated in air under quasi-isothermic and quasi-isobaric conditions [11] or in an atmosphere of ammonia [1,2]. Experiments carried out in ammonia atmosphere at various pressures p_{NH_3} have shown that the section of TG curve corresponding to the course of reaction (1) begins to appear at a definite value of p_{NH_3}, e.g. at $p_{NH_3} > 40$–50 hPa in the case of $M^{II} = Co$. At higher values of p_{NH_3}, the section broadens with increasing pressure, and at lower p_{NH_3} it disappears, the TG curve becoming similar to that obtained on heating $NH_4CoPO_4 \cdot H_2O$ in vacuum. Figure 6 shows such a curve recorded at $p_{NH_3} = 136$ hPa. Within the limits of that section corresponding to reaction (1) ($\theta = 270$–320°C), and also of the corresponding section on the TG curve obtained at $p_{NH_3} = 925$ hPa ($\theta = 320$–390°C), the sample is a high-temperature form of the anhydrous salt, the X-ray diffraction pattern of which corresponds to that of NH_4CoPO_4-**I** [1,3] (Fig. 7).

According to the chemical and X-ray structural analysis data within the limits of these sections, the samples of NH_4CoPO_4-**I** do not contain any products of anionic condensation or deammoniation of the sample material. The anhydrous ammonium cobalt phosphate formed under these conditions is relatively stable as compared with the analogous salts of manganese and copper. Figure 8 shows kinetic curves of the changes in phosphorus contents (in mass percent) in the form of monophosphate (P_1), diphosphate (P_2), and triphosphate (P_3) under isothermal heating of $NH_4M^{II}PO_4 \cdot H_2O$ (where M^{II} is Mn, Co, Cu) in an atmosphere of ammonia at $p_{NH_3} = 136$ hPa and $\theta = 310$°C. Up to the time of heating, $\tau = 1$ h in the case of Cu salt and $\tau = 2$ h for Co, the samples contained 100% P_1, whereas on heating

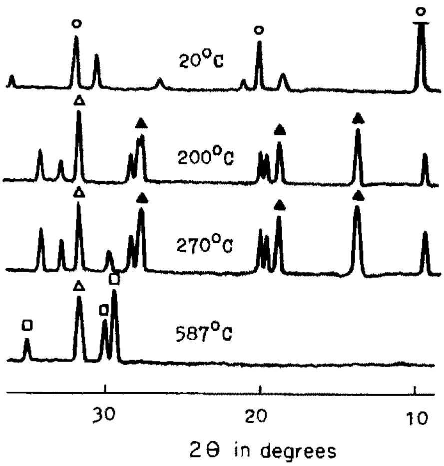

Fig. 7. X-ray diffraction patterns of $NH_4CoPO_4 \cdot H_2O$ and of the products of its thermal decomposition in gaseous ammonia atmosphere, $p_{NH_3} = 136$ hPa, HR = 2.5 K min^{-1}: ○, $NH_4CoPO_4 \cdot H_2O$; △, NaCl; ▲, NH_4CoPO_4-**I**; □, α-$Co_2P_2O_7$.

$NH_4MnPO_4 \cdot H_2O$ the anionic rearrangement started immediately, and within $\tau = 4$ h the P_1 content was reduced to 30%.

A feature of the heating of $NH_4CoPO_4 \cdot H_2O$ in an atmosphere of water vapour is that curve 2 (Fig. 5) intersects with curve 3 at low temperatures due to the known effect of impedance [17]; at high temperatures it passes above the curves 1 and 3. This is due to the mineralizing effect of water

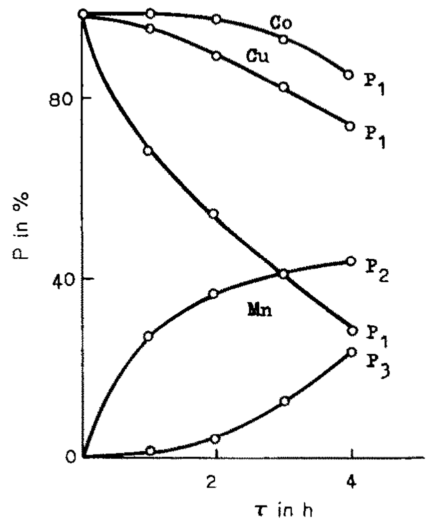

Fig. 8. Kinetic curves of $NH_4M^{II}PO_4 \cdot H_2O$ (where M^{II} is Mn, Co, Cu); anion rearrangement at $p_{NH_3} = 136$ hPa and $\theta = 310$°C.

vapour, which accelerates the crystallization of α-$Co_2P_2O_7$. The presence of water vapour lowers the temperature of the beginning of deammoniation, and also the temperature of the start of anionic condensation. According to literature data [4, 13], when $NH_4CoPO_4 \cdot H_2O$ is heated in open air, the first signs of anionic condensation appear at $\theta > 200°C$. In our experiments, a sample of $NH_4CoPO_4 \cdot H_2O$ heated isothermally for $\tau = 350$ min at 184°C in water vapour ($p_{H_2O} = 20$ hPa) contained 86.6% P_1 and 13.4% P_2. After heating for $\tau = 405$ min at 230°C, the sample contained 54.5% P_1, 41.3% P_2 and 4.2% P_3.

As the presence of water vapour suppresses the beginning of dehydration, the samples heated in an atmosphere of water vapour lose, in the first step, more ammonia than crystallization water. Thus, on isothermal heating of $NH_4CoPO_4 \cdot H_2O$ (at $p_{H_2O} = 20$ hPa) for 300 min at $\theta = 140°C$ (Table 1), the sample has lost 0.03 moles of NH_3 and no water; and on heating for 305 min at 150°C, it has lost 0.11 moles of NH_3 and 0.01 moles of H_2O. A further increase in temperature leads to an increase in the ratio $R = \text{mol } H_2O/\text{mol } NH_3$ lost. Above 168°C, the ratio becomes stabilized at $R = 1.5$–2.8 which is also the range for the values of R observed on

TABLE 1

Dehydration and deammoniation degree of $NH_4CoPO_4 \cdot H_2O$ heated under isothermal conditions

θ/°C	τ/min	Δm_{H_2O}/mol H_2O	Δm_{NH_3}/mol NH_3	R [a]
$p = 10^{-5}$ hPa				
109	300	0.22	0.14	1.6
118	300	0.43	0.21	2.0
130	630	0.81	0.46	1.8
138	300	0.75	0.40	1.9
157	412	1.14	0.58	2.0
178	300	1.14	0.71	1.6
195	300	1.25	0.73	1.7
215	308	1.27	0.76	1.7
267	300	1.35	0.77	1.8
310	300	1.44	0.80	1.8
$p_{H_2O} = 20$ hPa				
140	300	0	0.03	0
150	305	0.01	0.11	0.1
168	440	0.48	0.28	1.7
177	480	0.93	0.39	2.4
190	390	1.08	0.41	2.6
200	300	1.16	0.41	2.8
300	252	1.34	0.63	2.1
397	300	1.36	0.88	1.5

[a] R is mol H_2O/mol NH_3.

TABLE 2

Kinetic data for the isothermal dehydration and deammoniation of $NH_4M^{II}PO_4 \cdot H_2O$ at $p = 10^{-5}$ hPa

$NH_4MgPO_4 \cdot H_2O$				$NH_4MnPO_4 \cdot H_2O$			
τ/min	Δm_{H_2O}/ mol H_2O	Δm_{NH_3}/ mol NH_3	R	τ/min	Δm_{H_2O}/ mol H_2O	Δm_{NH_3}/ mol NH_3	R [a]
117°C				102°C			
40	0.04	0.02	2.0	12	0.05	0.02	2.5
60	0.08	0.04	2.0	60	0.10	0.05	2.0
80	0.12	0.06	2.0	95	0.17	0.07	2.4
100	0.17	0.08	2.1	130	0.23	0.10	2.3
140	0.24	0.11	2.2	170	0.28	0.12	2.3
214	0.35	0.18	1.9	206	0.33	0.15	2.2
274	0.44	0.24	1.8	250	0.39	0.18	2.2
133°C				140°C			
20	0.07	0.04	1.8	7	0.10	0.05	2.0
44	0.23	0.10	2.3	16	0.23	0.10	2.3
70	0.38	0.18	2.1	28	0.36	0.16	2.2
100	0.52	0.25	2.1	50	0.47	0.21	2.2
130	0.60	0.31	1.9	95	0.58	0.27	2.1
170	0.68	0.37	1.8	170	0.67	0.30	2.2
275	0.77	0.44	1.8	265	0.75	0.32	2.3
153°C				205°C			
11	0.26	0.10	2.6	10	0.80	0.27	3.0
24	0.48	0.22	2.2	26	0.89	0.36	2.5
43	0.71	0.36	2.0	30	1.01	0.42	2.4
140	1.00	0.55	1.8	50	1.12	0.47	2.4

[a] R is mol H_2O/mol NH_3.

dehydration and deammoniation of $NH_4CoPO_4 \cdot H_2O$ in vacuum, in the absence of a predominant removal of ammonia at lower temperatures.

The results of the studies on the kinetics of isothermal dehydration and deammoniation of $NH_4M^{II}PO_4 \cdot H_2O$ (where M^{II} is Mg and Mn) in vacuum have shown that in this case most values of R fall in the range 1.8–3.0 (Table 2). The values of R given in Table 2 relate to the stage of half deammoniation ($\Delta m_{NH_3} < 0.5$ mol NH_3) which proceeds in the kinetic region and may be characterized by the value of the kinetic parameter n in the equation $\alpha = 1 - \exp(-k'\tau^n)$ exceeding unity ($n > 1$) (α is the degree of transformation and k' is a constant). At $\Delta m_{NH_3} > 0.5$ mol NH_3, the process of deammoniation becomes diffusion-limited and the value of n falls below 0.5 ($n < 0.5$).

The decrease in n during the isothermal process reflects the change in the course of the kinetic curve. It corresponds to the completion of the kinetic

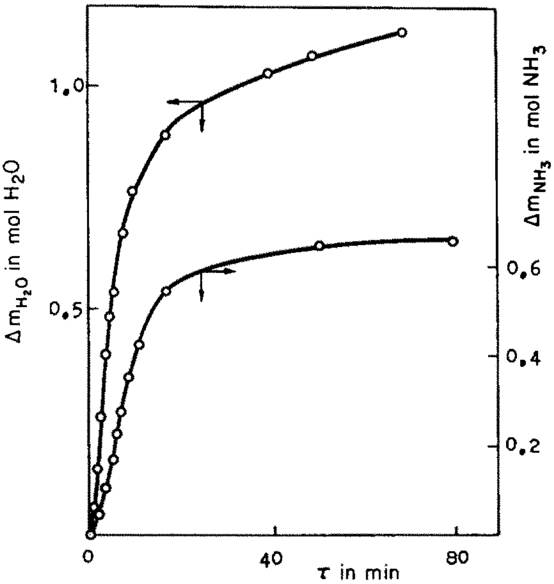

Fig. 9. Kinetic curves of $NH_4MgPO_4 \cdot H_2O$ dehydration and deammoniation at $p = 10^{-5}$ hPa and $\theta = 173°C$.

stage of the process and the change to the diffusion-controlled stage [18]. An example given in Fig. 9 shows the kinetic curves of dehydration and deammoniation of $NH_4MgPO_4 \cdot H_2O$ in vacuum at 173°C, where under conditions of the kinetic stage of deammoniation ($\Delta m_{MH_3} = 0.1$–0.5 mol NH_3) the parameter has the value of $n = 1.2$, whereas in the diffusion-controlled region ($\Delta m_{NH_3} > 0.5$ mol NH_3), $n = 0.4$. Analogously, for the process of dehydration, $n = 1.1$ for $\Delta m_{H_2O} = 0.1$–1.0 mol H_2O and $n = 0.3$ for $\Delta m_{H_2O} > 1$ mol H_2O.

The ratio of the durations of the kinetic and diffusion-controlled stages of the topochemical processes changes as a function of the size of the crystals [19]. In our experiments, as well as in the thermal decomposition of $Na_5P_3O_{10} \cdot 6H_2O$ [19–21], a reduction in the size of the crystals resulted in an extension of the first stage and a shortening of the diffusion-controlled stage. The extent of the influence of crystal size on the kinetics of the liberation of gas products can be evaluated from the data for $NH_4CoPO_4 \cdot H_2O$ given in Fig. 10. The sample of $NH_4CoPO_4 \cdot H_2O$ ($D = 0.1$–0.2 mm) was ground in a vibration grinder to obtain an average grain size in the range $D_1 = 0.005$–0.01 mm. By reducing the rate of crystallization of $NH_4CoPO_4 \cdot H_2O$ from the aqueous solution, we obtained a coarse grained sample, which was then sifted to obtain fractions of mean size $D_2 = 0.01$–0.02 mm and $D_3 = 0.8$–1.0 mm.

Comparison of the curves for D_2 and D_3 (Fig. 10) enables the increase in the rate of the overall process due to the decrease in the size of the crystals

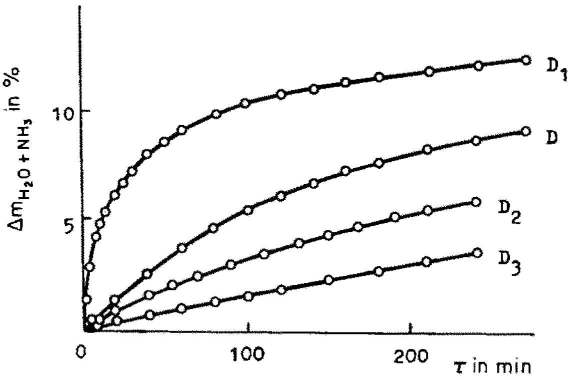

Fig. 10. Kinetic curves of $NH_4CoPO_4 \cdot H_2O$ thermal decomposition at $p = 10^{-5}$ hPa and $\theta = 130°C$: D, 0.1–0.2 mm; D_1, 0.005–0.01 mm; D_2, 0.01–0.02 mm; D_3, 0.8–1.0 mm.

precipitated from solution to be evaluated. Comparison of the curves for D_1 and D gives an estimation of the size reduction of the crystals as a consequence of mechanical grinding. Comparison of the curves for D and D_2 shows that, in addition to the degree of dispersion, the rate of crystal growth of the polycrystalline samples also influences the kinetics of thermal decomposition: rapidly grown, coarse grained crystals of $NH_4CoPO_4 \cdot H_2O$ are decomposed more rapidly (curve D) than slowly grown crystals that have not had enough time to become coarse grained (curve D_2).

CONCLUSION

The relationships between the rates of dehydration, deammoniation, and anion rearrangement during isothermal and non-isothermal heating of $NH_4M^{II}PO_4 \cdot H_2O$ (where M^{II} is Mg, Mn, Co, or Cu) in the temperature range $\theta = 20$–$950°C$, as well as between the durations of the kinetic and diffusion-controlled stages of the process, can be controlled by changing the composition and the pressure of the surrounding atmosphere, the degree of dispersion of the polycrystalline samples, and the means of changing the crystal size. When heating is carried out in an atmosphere of gaseous ammonia at a sufficient pressure, in particular at $p_{NH_3} > 40$–50 hPa in the case of $NH_4CoPO_4 \cdot H_2O$, it is possible to eliminate all the crystallization water with no loss of ammonia and without anionic condensation.

A feature of the thermal transformations in a vacuum of the materials under study (at $p = 10^{-5}$ hPa) is the simultaneous elimination of water and ammonia. The molar ratio of the water and ammonia lost during the kinetic step of the process does not leave the region of R (mol H_2O)/(mol NH_3) = 1.8–3.0 (where M^{II} is Mg or Mn).

When $NH_4CoPO_4 \cdot H_2O$ is heated in an atmosphere of water vapour ($p_{H_2O} = 20$ hPa), the beginning of gas evolution consists mainly in the elimination of ammonia. Then the value of R increases and attains

$R = 1.52$–2.8. The presence of water vapour lowers the temperature of the beginning of anionic condensation and accelerates the crystallization of the final product of the reaction, which is α-$Co_2P_2O_7$.

REFERENCES

1 J.-J. Etienne and A. Boulle, Bull. Soc. Chim. Fr., 5 (1969) 1534.

2 A.G. Ryadchenko and L.N. Shchegrov, Izv. Akad. Nauk SSSR, Neorg. Mater., 11 (1975) 2034 (in Russian).

3 Powder Diffraction File, Inorganic, 1972, Sets 22–42, 22–43.

4 J.-J. Etienne and A. Boulle, Bull. Soc. Chim. Fr., 4 (1968) 1805.

5 J.-J. Etienne and A. Boulle, C. R. Acad. Sci., 264 (1967) 1593.

6 J.-J. Etienne and A. Boulle, C. R. Acad. Sci., 260 (1965) 3977.

7 L.N. Shchegrov, V.V. Pechkovskii, A.G. Ryadchenko and R.Ya. Melnikova, Zh. Neorg. Khim., 16 (1971) 3056 (in Russian).

8 L. Erdey, G. Liptay, F. Paulik and S. Gal, Period. Politech. Chem. Eng., 5 (1961) 209.

9 J. Paulik and F. Paulik, J. Therm. Anal., 3 (1971) 63.

10 J. Paulik and F. Paulik, Thermochim. Acta, 4 (1972) 189.

11 J. Paulik and F. Paulik, J. Therm. Anal., 8 (1975) 567.

12 J. Paulik and F. Paulik, Simultaneous Thermoanalytical Examinations by Means of the Derivatograph, Part A, Elsevier/North Holland, New York, 1981, 277 pp.

13 L.N. Shchegrov, Fosfaty Dvukhvalentnykh Metallov (Phosphates of Divalent Metals), Naukova Dumka, Kiev, 1987, 214 pp. (in Russian).

14 Z.A. Konstant and A.P. Dindune, Fosfaty Dvukhvalentnykh Metallov (Phosphates of Divalent Metals), Zinatne, Riga, 1987, 371 pp. (in Russian).

15 Tranqui Duc, A. Durif, J.-C. Guitel and M.-T. Averbuch-Pouchot, Bull. Soc. Chim. Fr., 4 (1968) 1759.

16 J. Fraissard and J.-J. Etienne, Bull. Soc. Chim. Fr., 4 (1968) 1756.

17 W.E. Garner (Ed.), Chemistry of the Solid State, Buttterworths, London, 1955, pp. 215–220.

18 E.A. Prodan, Neorganicheskaya Topokhimiya (Inorganic Topochemistry), Nauka i Tekhnika, Minsk, 1986, pp. 153–160 (in Russian).

19 E.A. Prodan, Topokhimiya Kristalov (Topochemistry of Crystals), Nauka i Tekhnika, Minsk, 1990, p. 28, 63, 202 (in Russian).

20 V.M. Galogaza, E.A. Prodan, V.A. Sotnikova-Yuzhik, D.U. Skala, N.V. Bulavkina and S.I. Pytlev, Thermochim. Acta, 106 (1986) 141.

21 V.M. Galogaza, S.G. Tereshkova and E.A. Prodan, Thermochim. Acta, 142 (1989) 265.